Optimized Mappings for Iteratively Decoded BICM on Rayleigh Channels with IQ Interleaving

Thorsten Clevorn, Susanne Godtmann, and Peter Vary
Institute of Communication Systems and Data Processing (ind), RWTH Aachen University, Germany
clevorn@ind.rwth-aachen.de

***Abstract*— A cost function for the optimization of mappings for bit-interleaved coded modulation systems with iterative decoding (BICM-ID) for a Rayleigh channel with applied IQ interleaving is derived. For this channel model the optimum mapping depends on the channel quality and on the rotation of the signal constellation set. Simulation results reveal that mappings optimized with the new cost function yield a better performance than previously known mappings. Furthermore, a second, easy procedure to obtain the optimum rotation angle for a signal constellation set in conjunction with IQ Interleaving is described.**

I. Introduction

In digital communications the transmitted signal is often affected by fading due to, e.g., multi-path propagation. *Bit-interleaved coded modulation* (BICM) [1, 2] is a band-width efficient coded modulation scheme which increases the time-diversity and consequently is especially suited for Rayleigh fading channels. The key element of BICM is the serial concatenation of channel encoding, bit-interleaving, and multilevel modulations at the transmitter. In order to increase the performance of BICM in [3, 4] a feedback loop is added to the decoder, which results in a turbo-like decoding process. This new scheme is known as BICM with *iterative decoding* (BICM-ID). Another key element of BICM-ID is the usage of non-Gray mappings in the modulator. With these a significant improvement by the iterations can be achieved. By *mapping* we denote the whole design process of locating the possible positions of the channel symbols in the signal space, the *signal constellation set* (SCS), and assigning the possible bit patterns to these symbols.

A lot of research, e.g. [3–7], has been done to develop optimum mappings for different channels and SCSs. In this paper we derive an appropriate cost function for a Rayleigh channel with IQ interleaving [4, 6, 8]. With an IQ interleaver the in-phase (I) and quadrature (Q) component of a modulated symbol shall be made to fade independently to increase the signal space diversity [9]. It turns out that the optimum mapping depends on the channel quality and on the rotation of the SCS. Using the mutual information measure of extrinsic information transfer (EXIT) charts [10], a simple technique is proposed to obtain the optimum rotation angle. This method uses elements of the BER prediction for BICM-ID [11] based on EXIT charts, which is also outlined. Simulations results demonstrate the superiority of the mappings developed with the new cost function and the importance of choosing the correct rotation angle.

This work has been supported by the Deutsche Forschungsgemeinschaft DFG.

[1]Susanne Godtmann is now with the Institute for Integrated Signal Processing Systems, RWTH Aachen University

II. The BICM-ID System

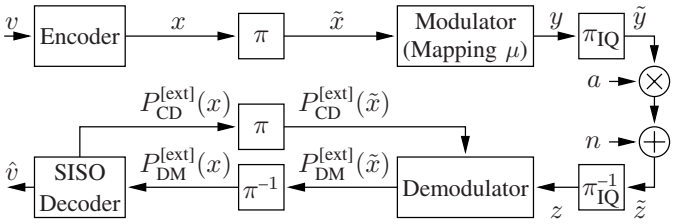

Fig. 1. Baseband model of the BICM-ID system

The baseband model of a BICM-ID system is depicted in Fig. 1. A frame of V information bits v is encoded by a standard non-systematic feed-forward convolutional encoder. The resulting encoded bits x are permuted by a pseudo-random bit-interleaver π to $\tilde{x}$. According to a mapping μ the modulator maps the interleaved bits $\tilde{x}$ in bit patterns $\tilde{\mathbf{x}}$ (comprising I bits) to a complex channel symbol $y \in \mathbb{C}$ out of the signal constellation set (SCS) $\mathcal{Y}$. As channel model we consider the memoryless Rayleigh channel with fading coefficients a and AWGN n.

At the receiver, the channel decoder and the demodulator exchange extrinsic information in a Turbo process. The demodulator (DM) computes extrinsic probabilities $P_{\mathrm{DM}}^{[\mathrm{ext}]}(\tilde{x})$ for each bit $\tilde{x}_t^{(i)}$ being $b \in \{0,1\}$ according to [3]

$$P_{\mathrm{DM}}^{[\mathrm{ext}]}(\tilde{x}_t^{(i)}=b) \sim \sum_{\hat{y}\in\mathcal{Y}_b^i} P(z_t|\hat{y}) \prod_{j=1,j\neq i}^{I} P_{\mathrm{CD}}^{[\mathrm{ext,enc}]}\left(\tilde{x}_t^{(j)}=\mu^{-1}(\hat{y})^{(j)}\right) \quad (1)$$

Each $P_{\mathrm{DM}}^{[\mathrm{ext}]}(\tilde{x})$ consists of the sum over all possible channel symbols $\hat{y}$ for which the i^{th} bit of the corresponding bit pattern $\underline{\tilde{x}} = \mu^{-1}(\hat{y})$ is b. These channel symbols form the subset $\mathcal{Y}_b^i$ with $\mathcal{Y}_b^i = \{\mu([\tilde{x}^{(1)}, \ldots \tilde{x}^{(I)}]) | \tilde{x}^{(i)} = b\}$. In the first iteration the feedback probabilities $P_{\mathrm{CD}}^{[\mathrm{ext}]}(\tilde{x})$ are initialized as equiprobable, i.e., $P_{\mathrm{CD}}^{[\mathrm{ext}]}(\tilde{x}) = 0.5$. The conditional probability density $P(z_t|\hat{y}) = (1/\pi\sigma_n^2)\exp(-d_{z\hat{y}}^2/\sigma_n^2)$ with $d_{z\hat{y}}^2 = \|z_t - a_t\hat{y}\|^2$ describes the complex channel.

After appropriately deinterleaving the $P_{\mathrm{DM}}^{[\mathrm{ext}]}(\tilde{x})$ to $P_{\mathrm{DM}}^{[\mathrm{ext}]}(x)$, the $P_{\mathrm{DM}}^{[\mathrm{ext}]}(x)$ are fed into a Soft-Input Soft-Output (SISO)

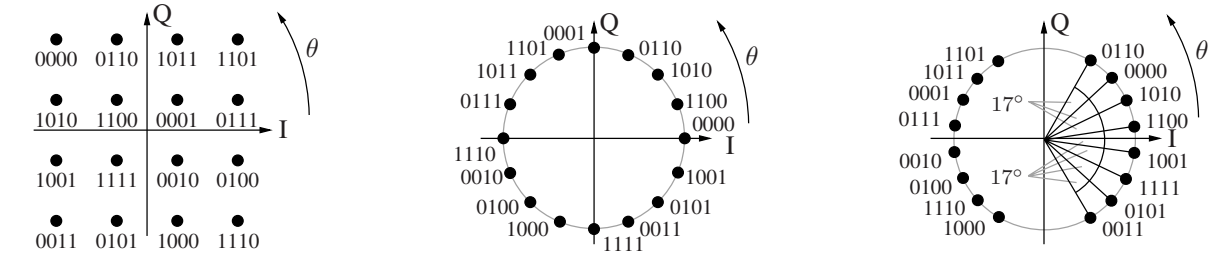

(a) 16QAM-IQ$_{10\text{dB}}$, $\theta_{\text{opt}}=0°$ (b) 16PSK-IQ$_{10\text{dB}}$, $\theta_{\text{opt}}=11.25°$ (c) 17°-16PSK-IQ$_{10\text{dB}}$, $\theta_{\text{opt}}=0°$

Fig. 2. Optimum mappings μ and rotation angles θ for a Rayleigh channel with IQ interleaving, $E_s/N_0=10$ dB.

channel decoder (CD), which computes extrinsic probabilities $P_{\text{CD}}^{[\text{ext}]}(x_t^{(i)})$ for the encoded bits $x_t^{(i)}=\{0,1\}$ in addition to the preliminary estimated decoded data bits $\hat{u}$. For the next iteration the $P_{\text{CD}}^{[\text{ext}]}(x)$ are interleaved again to $P_{\text{CD}}^{[\text{ext}]}(\tilde{x})$ in order to be fed into the demodulator. Note, in all steps of the receiver L-values (log-likelihood ratios) can be used instead of probabilities $P(\cdot)$.

To achieve a noticeable iterative gain by BICM-ID, other mappings than Gray mapping must be used [3]. For Rayleigh fading channels, the relevant criterion regarding the error floor (the asymptotic behavior) is the *harmonic mean* $\check{d}_h^2(\mu)$

$$\check{d}_h^2(\mu)=\left(\frac{1}{I2^I}\sum_{i=1}^{I}\sum_{b=0}^{1}\sum_{y\in\mathcal{Y}_b^i}\frac{1}{\|y-\check{y}\|^2}\right)^{-1} \tag{2}$$

of the *squared Euclidean decision distances* $\|y-\check{y}\|^2$ which occur for error-free feedback (EFF), i.e., $P_{\text{CD}}^{[\text{ext}]}(\tilde{x})\in\{0.0,1.0\}$. The channel symbol $\check{y}$ possesses the identical bit pattern as y, except for an inverted bit $b\in\{0,1\}$ at position i. To obtain the lowest possible error floor, $\check{d}_h^2(\mu)$ has to maximized. We refer to the literature for details. Numerous publications using $\check{d}_h^2(\mu)$ exist, e.g. [3–7], some considering the inverse

$$\check{D}^{[\text{Ray}]}(\mu)=\frac{1}{\check{d}_h^2(\mu)}=\frac{1}{I2^I}\sum_{i=1}^{I}\sum_{b=0}^{1}\sum_{y\in\mathcal{Y}_b^i}\frac{1}{\|y-\check{y}\|^2} \quad . \tag{3}$$

III. IQ Interleaving

The performance of BICM-ID on a Rayleigh channel can be further improved by exploiting the signal space diversity [9] with IQ interleaving [4, 6, 8]. The IQ interleaver π_{IQ} shall facilitate an independent fading of the in-phase (I) and quadrature (Q) components of a modulated symbol y. For a memoryless fading channel a simple wraparound shift by one symbol of the Q component is sufficient [4]:

$$\tilde{y}_t=\begin{cases}\text{Re}\{y_t\}+j\cdot\text{Im}\{y_{t-1}\} & 2\le t\le T\\ \text{Re}\{y_t\}+j\cdot\text{Im}\{y_T\} & t=1\end{cases} \quad . \tag{4}$$

However, with separate interleaving of the I and Q component the performance is not anymore invariant to a rotation of the SCS [4, 8]. Taking the IQ interleaving into account for the optimization, we derived the new cost function $\check{D}^{[\text{IQ}]}(\mu)$, which has to be minimized,

$$\check{D}^{[\text{IQ}]}(\mu)=\frac{1}{I2^I}\sum_{i=1}^{I}\sum_{b=0}^{1}\sum_{y\in\mathcal{Y}_b^i}\left(\frac{1}{1+\frac{E_s}{4N_0}(\text{Re}\{y-\check{y}\})^2}\right)\left(\frac{1}{1+\frac{E_s}{4N_0}(\text{Im}\{y-\check{y}\})^2}\right). \tag{5}$$

Similar to (2) the derivation of (5) is based on the pair-wise error probability (PEP) $P(x\to\check{x})$ [12]. For details to (2) see [2–4]. The bit-wise PEP for a Rayleigh channel is

$$P^{[\text{Ray}]}(x\to\check{x})\le\frac{1}{1+\|y-\check{y}\|^2/4N_0}\approx\frac{1}{\|y-\check{y}\|^2/4N_0}, \tag{6}$$

with the approximation valid for high SNRs, $1\ll\|y-\check{y}\|^2/4N_0$. With perfect IQ interleaving two independent Rayleigh fading channels (one for each of the two signal-space dimensions) exist, yielding a bit-wise PEP of

$$P^{[\text{IQ}]}(x\to\check{x})\le\left(\frac{1}{1+\frac{\text{Re}\{y-\check{y}\}^2}{4N_0}}\right)\left(\frac{1}{1+\frac{\text{Im}\{y-\check{y}\}^2}{4N_0}}\right) \quad . \tag{7}$$

Note, the approximation for high SNRs made in (6) is not useful here, since we would then get $P(x\to\check{x})\to\infty$ if $\text{Re}\{y-\check{y}\}=0$ or $\text{Im}\{y-\check{y}\}=0$.

The cost function $\check{D}^{[\text{IQ}]}(\mu)$ can now be used in a search algorithm such as a binary switching algorithm [5] or the exhaustive search algorithm presented in [6], which ensures a global optimum. Note, beside its dependency via $\text{Re}\{y-\check{y}\}$ and $\text{Im}\{y-\check{y}\}$ on the rotation of the SCS around the origin, $\check{D}^{[\text{IQ}]}(\mu)$ has an additional dependency on the channel quality E_s/N_0, similar to the cost function for a simple AWGN channel (see, e.g. [5, 6]). Analysis tools for this dependency are presented in [6].

IV. Simulation Results

The optimum mappings μ and rotation angles θ (assumed counter-clockwise) for some SCSs, e.g., standard 16QAM, 16PSK (which was found to be more suited for BICM-ID than 16QAM [6]), and the non-regular SCS 17°-16PSK [6, 13], are given in Fig. 2. These new mappings were optimized using $E_s/N_0=10$ dB, which corresponds to $E_b/N_0\approx 7$ dB with $I=4$ bit and the used rate-1/2 convolutional code with generator polynomials $\{15,17\}_8$. In Fig. 3 BER simulations are presented which show the advantage of mappings optimized

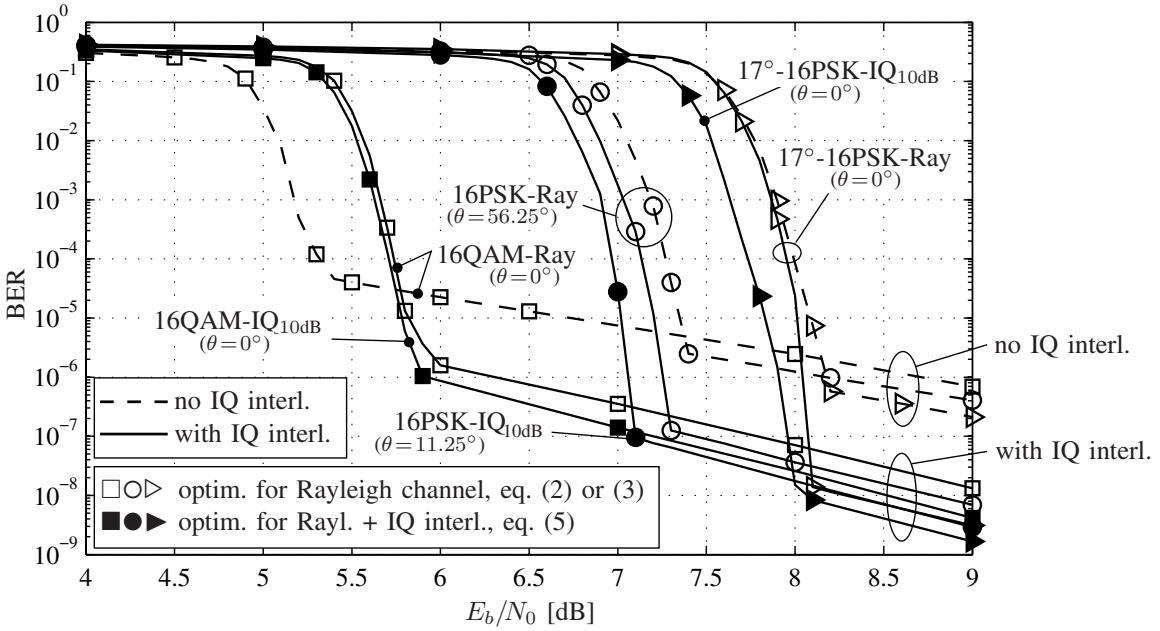

Fig. 3. BER for BICM-ID with 30 iterations, an 8-state, rate-1/2 convolutional code, $V=12000$ information bits per frame, and a Rayleigh fading channel.

for IQ interleaving using (5) (suffix "-IQ$_{E_s/N_0}$", filled markers) over mappings optimized for a regular Rayleigh channel with (2) (suffix "-Ray", non-filled markers). All mappings show a significant improvement of the error floor when IQ interleaving is applied (solid lines) compared to the case without IQ interleaving (dashed lines). However, the new mappings optimized with (5) outperform the previously known mappings [5, 6] (optimized using (2)) by up to ≈ 0.6 dB and exhibit also a better waterfall behavior. For each mapping the optimum SCS rotation angle θ (see also Section VI) at this E_s/N_0 is given in Fig. 3.

V. BER Prediction using EXIT Charts

EXIT charts [10] are a powerful tool to analyze and optimize the convergence behavior of iterative systems utilizing the Turbo principle, i.e., systems exchanging and refining extrinsic information. The capabilities of the components, in our case the demodulator (DM) and the channel decoder (CD), are analyzed separately. The extrinsic mutual information $\mathcal{I}^{[\text{ext}]}$ obtained by each component for a certain a priori mutual information $\mathcal{I}^{[\text{apri}]}$ is determined. Both, $\mathcal{I}^{[\text{ext}]}$ and $\mathcal{I}^{[\text{apri}]}$, are calculated on the basis of the actual bits, e.g., x, and the available information, extrinsic or a priori, for these bits. As basis for this calculation usually histograms of the respective L-values, e.g., $L_{\text{DM}}^{[\text{ext}]}$ of $P_{\text{DM}}^{[\text{ext}]}$ for $\mathcal{I}_{\text{DM}}^{[\text{ext}]}$, are used. For the EXIT characteristics the a priori L-values are simulated as uncorrelated Gaussian distributed, with variance σ_A^2 and mean $\mu_A=\sigma_A^2/2$. The convergence behavior of BICM-ID has been studied, e.g., in [13].

In [11] the capabilities of the EXIT chart are extended to the prediction of BERs P_b for BICM-ID, as proposed for Turbo codes in [10]. However, the adaptation is not straightforward because in contrast to [10] the mutual information on the data bits u, $\mathcal{I}_{\text{CD}}^{[\text{ext,dec}]}$, is not used in the EXIT chart, but the mutual information on the encoded bits x, $\mathcal{I}_{\text{CD}}^{[\text{ext,enc}]}$. In Fig. 4 the EXIT characteristics for an 8-state, rate-1/2, feed-forward convolutional code with generator polynomials $\{15, 17\}_8$ and for 8PSK-SP (set-partitioning) mapping [3] are depicted. The EXIT characteristic of the demodulator, $\mathcal{I}_{\text{DM}}^{[\text{ext}]}=f(\mathcal{I}_{\text{DM}}^{[\text{apri}]})$, depends on the channel quality, while the channel decoder characteristic, $\mathcal{I}_{\text{CD}}^{[\text{ext,enc}]}=f(\mathcal{I}_{\text{CD}}^{[\text{apri,enc}]})$, is independent of E_b/N_0, because the only input for the decoder is $P_{\text{DM}}^{[\text{ext}]}(x)$. Thus, also $\mathcal{I}_{\text{CD}}^{[\text{ext,dec}]}$, and consequently the BER P_b of the data bits u, depend solely on $\mathcal{I}_{\text{CD}}^{[\text{apri,enc}]}=\mathcal{I}_{\text{DM}}^{[\text{ext}]}$. The points "○" mark the intersections between the EXIT characteristics of demodulator and channel decoder and the points "□" mark the EXIT characteristics of the demodulator at $\mathcal{I}_{\text{DM}}^{[\text{apri}]}=1$ bit (cmp. Fig. 6).

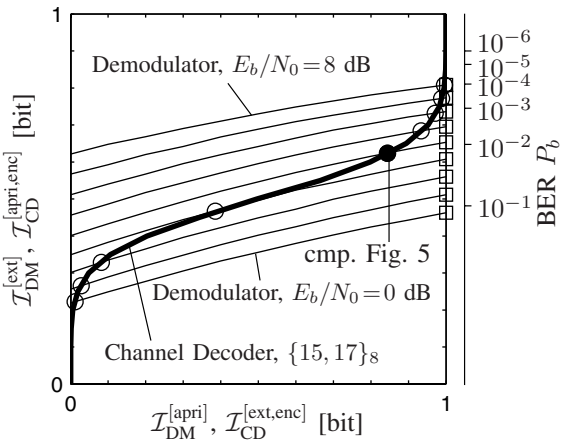

Fig. 4. EXIT characteristics for 8PSK-SP, Rayleigh channel

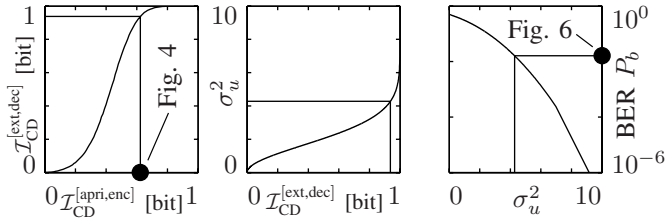

Fig. 5. The steps for BER prediction ("●" example for 8PSK-SP at 4 dB)

With the additionally measured EXIT characteristic $\mathcal{I}_{\text{CD}}^{[\text{ext,dec}]} = f(\mathcal{I}_{\text{CD}}^{[\text{apri,enc}]})$ for the decoded output of the decoder (Fig. 5, left plot) and the assumption of a Gaussian distributed decoder output $L_{\text{CD}}^{[\text{ext}]}(u)$ with variance σ_u^2 [10] we can stepwise calculate the BER. As example in Fig. 5 we use 8PSK-SP mapping at $E_b/N_0 = 4$ dB (point "●" in Figs. 4 and 6).

- Using the respective EXIT characteristic we can obtain $\mathcal{I}_{\text{CD}}^{[\text{ext,dec}]}$ for a given $\mathcal{I}_{\text{CD}}^{[\text{apri,enc}]} = \mathcal{I}_{\text{DM}}^{[\text{ext}]}$ (Fig. 5, left plot).
- With the inverse relation $\sigma_u \approx J^{-1}(\mathcal{I}_{\text{CD}}^{[\text{ext,dec}]})$ (this function cannot be expressed in closed form; for details see [10]) the variance σ_u^2 is computed (Fig. 5, center plot).
- Finally, the BER P_b is calculated as $P_b = \frac{1}{2}\operatorname{erfc}\left(\frac{\sigma_u^2}{2\sqrt{2}}\right)$ (Fig. 5, right plot)

On the right side of Fig. 4 a second axis for the BER is added. As already discussed before, the BER is independent of $\mathcal{I}_{\text{CD}}^{[\text{ext,enc}]} = \mathcal{I}_{\text{DM}}^{[\text{apri}]}$. Thus, in contrast to the systems in [10] for the considered BICM-ID system the curves of constant BER are simply horizontal lines (not depicted in Fig. 4).

In Fig. 6 the predicted BERs are compared with simulated BERs for the 8-state convolutional code of Fig. 4 and 8PSK-SP and 8PSK-SSP (semi-set-partitioning) mappings [3]. The block size is 12000 data bits per frame and 30 iterations are performed at the receiver. For infinite block size, a perfect interleaver, and a sufficient number of iterations the decoding trajectory should reach the intersection of the channel decoder characteristic and the demodulator characteristic in the EXIT chart. In Fig. 4 these points are marked by "○" for the depicted characteristics. As visible in Fig. 6 the corresponding estimated BERs (dashed curve "○") quite well match the simulated BERs (solid curve) in the whole depicted E_b/N_0-range. The waterfall-region as well as the error floor are accurately predicted, providing a simple design tool for BICM-ID systems for all channel conditions.

A key feature for the analysis of BICM-ID is the error floor [3, 5, 6]. In [6, 13] it was shown that the error floor can be analyzed using the EXIT chart. For the analysis of the error floor, error-free feedback (EFF) for the demodulator is assumed (for details see, e.g., [3]). This EFF is similar to perfect a priori knowledge, i.e., $\mathcal{I}_{\text{DM}}^{[\text{apri}]} = 1$ bit. Thus, the asymptotic behavior, i.e., the error floor, can be analyzed using the right axis of the EXIT chart [6, 13]. Consequently, for estimation of the error floor of the BER we have to use the demodulator characteristics at $\mathcal{I}_{\text{DM}}^{[\text{apri}]} = 1$ bit (points marked "□" in Fig. 4). Furthermore, a nice feature is that these points with $\mathcal{I}_{\text{DM}}^{[\text{apri}]} = 1$ bit can also be evaluated numerically, see

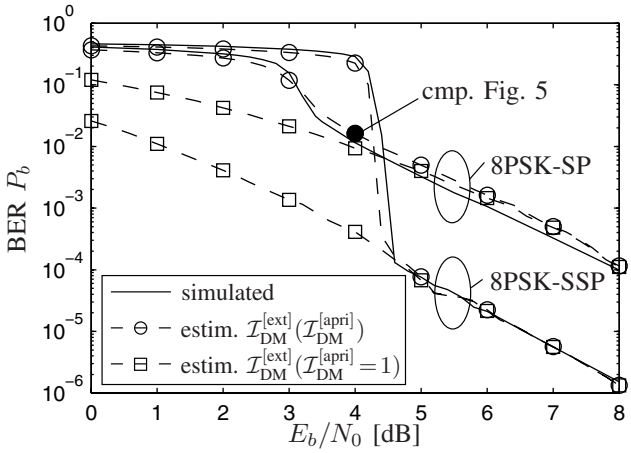

Fig. 6. Simulated and predicted BERs, 8-state conv. code, Rayleigh channel

e.g. [13], instead of using extensive Monte-Carlo simulations. The respective curve for the BER in Fig. 6 (dashed curve marked "□") shows that also the asymptotic behavior alone is very well predicted. Comparing Figs. 4 and 6 reveals that the BER for 8PSK-SP reaches the error floor at $E_b/N_0 \approx 4$ dB, corresponding to only $\mathcal{I}_{\text{DM}}^{[\text{apri}]} \approx 0.85$ bit, indicating that (in this case) already for $\mathcal{I}_{\text{DM}}^{[\text{apri}]} > 0.85$ bit the feedback can be considered as quasi error-free.

The curves for 8PSK-SSP (see Fig. 7) in Fig. 6 demonstrate that the proposed BER estimation is accurate for BERs down to at least 10^{-6}. In contrast, the BER prediction for Turbo codes in [10] is only reliable for BERs down to 10^{-3}.

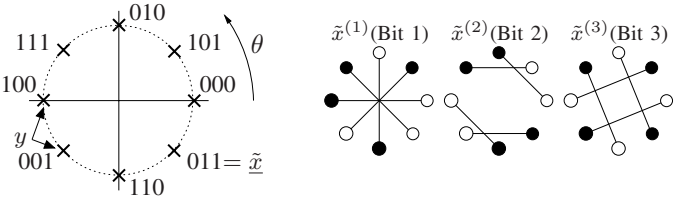

Fig. 7. 8PSK-SSP mapping [3] with EFF decision distances.

VI. Optimum Rotation Angles using EXIT charts

Using elements of the BER prediction method proposed in Section V, we will in the following present a simple method for obtaining the optimum rotation angle θ for a mapping, when the signal space diversity is exploited by IQ interleaving for a Rayleigh channel [11]. At first, we consider exemplarily the 8PSK-SSP mapping [3] (Fig. 7).

The error floor performance of BICM-ID is directly related to the decision distances for the EFF case, shown for 8PSK-SSP in Fig. 7 (right side). With IQ interleaving these distances shall not lie vertically or horizontally, but rather have large I and Q components. Examining the error floor we plot $\mathcal{I}_{\text{DM}}^{[\text{ext}]}(\mathcal{I}_{\text{DM}}^{[\text{apri}]} = 1)$ for different rotation angles θ in Fig. 8. Note that, e.g., for the optimization of θ for non-iterative BICM you would use $\mathcal{I}_{\text{DM}}^{[\text{ext}]}(\mathcal{I}_{\text{DM}}^{[\text{apri}]} = 0)$. As visible the highest $\mathcal{I}_{\text{DM}}^{[\text{ext}]}$ is obtained for $\theta = 22.5°$, the lowest for $\theta = 67.5°$. Intuitively,

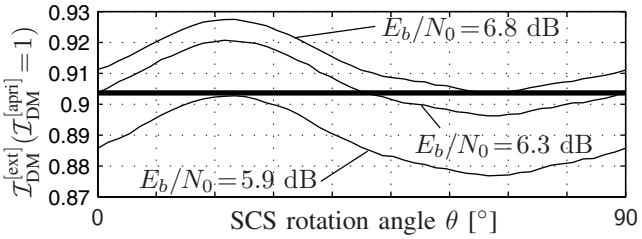

Fig. 8. $\mathcal{I}_{\mathrm{DM}}^{[\mathrm{ext}]}(\mathcal{I}_{\mathrm{DM}}^{[\mathrm{apri}]}=1)$ vs. rotation angle θ for 8PSK-SSP mapping.

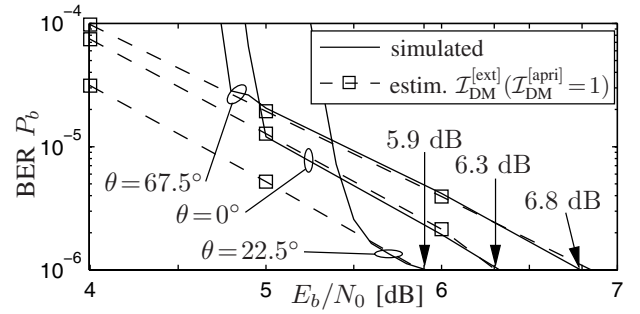

Fig. 9. Simulated and predicted BERs, 8-state conv. code, 8PSK-SSP, Rayleigh channel with IQ interleaving

with $\theta = 22.5°$ all distances for bits 1 and 2 have non-zero I and Q components and the distances for bit 3 even feature identical I and Q components resulting in a good performance. In contrast, for $\theta = 67.5°$ the decision distances of bit 3 are parallel to the I or Q axis (I or Q component is zero), with bits 1 and 2 being principally similar to the $\theta = 22.5°$ case.

With $\mathcal{I}_{\mathrm{CD}}^{[\mathrm{apri,enc}]} = \mathcal{I}_{\mathrm{DM}}^{[\mathrm{ext}]}$ the differences in required E_b/N_0 for a certain $\mathcal{I}_{\mathrm{DM}}^{[\mathrm{ext}]}$ are directly related to the BER as shown in Fig. 9. The mentioned E_b/N_0 correspond to a BER of 10^{-6}, i.e., $\mathcal{I}_{\mathrm{DM}}^{[\mathrm{ext}]} \approx 0.904$ in Fig. 8, for the respective rotation angle θ.

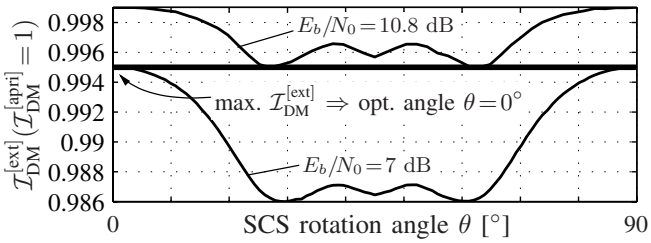

Fig. 10. $\mathcal{I}_{\mathrm{DM}}^{[\mathrm{ext}]}(\mathcal{I}_{\mathrm{DM}}^{[\mathrm{apri}]}=1)$ vs. angle θ for 16QAM-IQ$_{\mathrm{10dB}}$ mapping.

The result for 16QAM-IQ$_{\mathrm{10dB}}$ is depicted in Fig. 10. The maximum $\mathcal{I}_{\mathrm{DM}}^{[\mathrm{ext}]}$ is obtained for $\theta = 0° + k90°$, $k \in \mathbb{Z}$. The two curves are for $E_b/N_0 = 7$ dB and $E_b/N_0 = 10.8$ dB. Thus, in this case the performance can decrease by up to $\Delta_{E_b/N_0} = 3.8$ dB with a wrong rotation angle θ.

VII. Summary

We derived a new cost function for the optimization of mappings for BICM-ID when a Rayleigh channel with IQ interleaving is used. Contrariwise to a standard Rayleigh channel, the optimum mapping depends on the channel quality and potentially requires a rotated SCS. Simulation results show that the new mappings noticeably outperform the ones previously known, which were optimized for a Rayleigh channel without IQ interleaving. Furthermore, we presented a second tool based on EXIT charts to determine the optimum rotation angle. This latter method is based on the analytic prediction of the BER of BICM-ID using EXIT charts, which is also outlined in this paper.

References

[1] E. Zehavi, "8-PSK Trellis Codes for a Rayleigh Channel," *IEEE Trans. Comm.*, pp. 873–884, May 1992.

[2] G. Caire, G. Taricco, and E. Biglieri, "Bit-Interleaved Coded Modulation," *IEEE Trans. Inform. Theory*, pp. 927–946, May 1998.

[3] X. Li, A. Chindapol, and J. A. Ritcey, "Bit-Interleaved Coded Modulation With Iterative Decoding and 8PSK Signaling," *IEEE Trans. Comm.*, pp. 1250–1257, Aug. 2002.

[4] A. Chindapol and J. A. Ritcey, "Design, Analysis, and Performance Evaluation for BICM-ID with Square QAM Constellations in Rayleigh Fading Channels," *IEEE J. Select. Areas Commun.*, May 2001.

[5] F. Schreckenbach, N. Görtz, J. Hagenauer, and G. Bauch, "Optimized Symbol Mappings for Bit-Interleaved Coded Modulation with Iterative Decoding," in *IEEE Globecom*, San Francisco, CA, USA, Dec. 2003.

[6] T. Clevorn, S. Godtmann, and P. Vary, "PSK versus QAM for Iterative Decoding of Bit-Interleaved Coded Modulation," in *IEEE Globecom*, Dallas, TX, USA, Dec. 2004.

[7] J. Tan and G. L. Stüber, "Analysis and Design of Sympol Mappers for Iteratively Decoded BICM," *IEEE Trans. Wireless Comm.*, pp. 662–672, Mar. 2005.

[8] A. Chindapol and J. A. Ritcey, "BICM with Signal Space Diversity: Bounds for Rotated BICM and BICM-ID," in *CISS 2000*, Princeton, NJ, USA, Mar. 2000.

[9] J. Boutros and E. Viterbo, "Signal Space Diversity: A Power- and Bandwidth-Efficient Diversity Technique for the Rayleigh Fading Channel," *IEEE Trans. Inform. Theory*, pp. 1453–1467, July 1998.

[10] S. ten Brink, "Convergence Behavior of Iteratively Decoded Parallel Concatenated Codes," *IEEE Trans. Comm.*, pp. 1727–1737, Oct. 2001.

[11] T. Clevorn, S. Godtmann, and P. Vary, "BER prediction using EXIT charts for BICM with iterative decoding," *IEEE Comm. Lett.*, pp. 49–51, Jan. 2006.

[12] S. Benedetto and E. Biglieri, *Principles of Digital Transmission: With Wireless Applications*. Kluwer Academic / Plenum Publishers, 1999.

[13] T. Clevorn, S. Godtmann, and P. Vary, "EXIT Chart Analysis of Non-Regular Signal Constellation Sets for BICM-ID," in *ISITA 2004*, Parma, Italy, Oct. 2004.